Electrical Interactions via the Extracellular Potential Near Cell Bodies

Gary R. Holt*,† and Christof Koch*

20 August, 1998

* Computation and Neural Systems Program
California Institute of Technology
Pasadena, CA 91125

† Please address all correspondence to:
Dr. Gary Holt
Biomedical Engineering Department
University of Southern Californa
MC 1451
Los Angeles, CA 90089
Phone: (213)-740-3397
FAX: (213)-740-0343
email: holt@lnc.usc.edu

Abstract

Ephaptic interactions between a neuron and axons or dendrites passing by its cell body can be, in principle, more significant than ephaptic interactions among axons in a fiber tract. Extracellular action potentials outside axons are small in amplitude and spatially spread out, while they are larger in amplitude and much more spatially confined near cell bodies.

We estimated the extracellular potentials associated with an action potential in a cortical pyramidal cell using standard 1-D cable and volume conductor theory. Their spatial and temporal pattern reveal much about the location and timing of currents in the cell, especially in combination with a known morphology, and simple experiments could resolve questions about spike initiation. From the extracellular potential we compute the ephaptically induced polarization in a nearby passive cable. The magnitude of this induced voltage can be several mV, does not spread electrotonically and depends only weakly on the passive properties of the cable. We discuss their possible functional relevance.

Keywords

- extracellular field potential
- volume conduction
- branch point failure
- axon hillock/initial segment

1 Introduction

Neuroscientists usually assume that neurons communicate only through anatomical specializations such as gap junctions or synapses. The output of the neuron is thought to be completely determined if the synaptic inputs are specified. The goal of biophysical modeling has been to calculate and to understand how this output depends on the synaptic input.

Is the extracellular environment sufficiently constant that we can make this approximation? Only a small fraction (usually about 20%) of the space in the brain is actually extracellular (Nicholson, 1995; Syková, 1997). There is sometimes only about 20 nm between one cell membrane and the membrane of its neighbor (the average distance is somewhat larger; Van Harreveld, 1972). A single spike from a neuron can cause an extracellular potential of a few mV near the cell body. How much of an effect does this have on nearby neural elements?

Studies on squid giant axons (Arvanitaki, 1942), crab motoneurons (Katz and Schmitt, 1942), frog sciatic nerve (Kocsis *et al.*, 1982), and even algal strands (Tabata, 1990) showed that when two axons were placed in a medium with reduced extracellular conductance, activity in one axon could depolarize the other. (See also Bullock, 1965 and references therein.) Such interactions are called *ephaptic* (Greek "touching onto", rather than *synaptic*, "touching together"; Arvanitaki, 1942). The early studies were done before the chemical nature of synaptic transmission in the central nervous system was understood, and were thought to be evidence that transmission could be purely electrical (see Eccles, 1964; Faber and Korn, 1989). In extreme cases an action potential can be induced in an inactive axon by a nearby one. In fact, ephaptic transmission may underly pathological activity in motoneurons in some kinds of facial spasms, or in crushed nerves or in nerves damaged by multiple sclerosis (see Faber and Korn, 1989; Jefferys, 1995).

There have been only two demonstrations of electrical ephaptic effects in normal operations: between the Mauthner cell and its inhibitory afferents (Korn and Faber, 1980; Faber and Korn, 1989), and between basket cells and Purkinje cells in the cerebellum (Korn and Axelrad, 1980). Both of these systems have specific properties that enhance the magnitude of ephaptic effects (in the former, an unusually resistive extracellular space; in the latter, tight junctions around the synapse). There has been no clear evidence for ephaptic interactions in healthy systems without such unusual properties. Several studies have shown significant effects of field potentials in response to electrical stimulation, when many neurons are simultaneously active (Dalkara *et al.*, 1986; Turner and Richardson, 1991), but so far no interactions without electrical stimulation are known except in epilepsy (Snow and Dudek, 1984; Traub *et al.*, 1985a, 1985b).

Most theoretical studies of ephaptic interactions have examined parallel axons, because the geometry is simple and easy to analyze (Clark and Plonsey, 1970, 1971; Markin, 1970a, 1970b, 1973a; Scott and Luzader, 1979; Barr and Plonsey, 1992). Because the currents involved in axonal action potential propagation are small, an axon in normal tissue has an extracellular potential of only a few μV (e.g., Clark and Plonsey, 1968; Rosenfalck, 1969). However, an axon in a resistive sheath such as the perineurium surrounding peripheral

nerve axon bundles can have a somewhat larger potential because of the reduced extracellular volume. The extracellular space can be treated as approximately one-dimensional (the "core-conductor" approximation; Trayanova *et al.*, 1990). Action potentials in different fibers tend to phase-lock slightly out of step, and the propagation velocity can be slightly altered. However, these ephaptic interactions amount to only minor perturbations in the timing of action potentials; significant effects are seen only when many fibers are simultaneously stimulated (Nelson, 1966). Under normal physiological conditions, new action potentials are probably never created and already propagating potentials are never blocked.

Much less attention has been given to ephaptic interactions around cell bodies. This is somewhat surprising since the potentials can be considerably larger (up to a maximum of 3–5 mV; e.g., see the potentials in Fatt, 1957; Freygang and Frank, 1959; Terzuolo and Araki, 1961; Rosenthal, 1972). Potentials around cell bodies are not well understood, and analysis is complicated by the irregular geometry of dendrites. An approximate theory based on the concepts of "closed fields" (a spherically symmetric distribution of current sources/sinks) and "open fields" (an asymmetric distribution) can explain many features of extracellular recordings (Bishop and O'Leary, 1942; Lorente de Nó, 1947; see Hubbard *et al.*, 1969, ch. 7 for a review). Rall (1962) has used the closed field and equivalent cylinder approximations to estimate the magnitude of the extracellular action potential for stellate motoneurons. We are unaware of other efforts to compute the shapes of the extracellular action potentials near the cell body.

In order to understand how potentials near a cell body can affect other nearby neurons, we computed the potential directly from a detailed compartmental model that includes the full complexity of the dendritic geometry. We then analyzed how the resulting extracellular potential influences axons or dendrites near the cell body. Electric potentials are much more spatially confined near cell bodies than around axons. As a result, the mode of ephaptic interaction is qualitatively different. Interaction near cell bodies could potentially be more important than interaction between axons.

Other forms of non-synaptic interaction between neurons are known or possible. For example, slow potentials in the brain due to summed electrical activity of many neurons may be large enough to influence neural behavior (e.g., Bullock, 1997). Similarly, changes in extracellular ion concentration accompany neural activity and may noticeably influence nearby neurons. This paper does not attempt to address these potentially significant issues; we focus exclusively on the electrical effect of one neuron's spike on nearby neurons.

2 Methods

The effect of a spike in a neuron on an adjacent axon/dendrite was calculated in three stages. First, we computed the transmembrane currents for a pyramidal neuron model on the basis of standard 1-D cable theory. Second, we used those currents to compute the extracellular potentials. Third, we used the computed extracellular potentials to compute the transmembrane potential of a cable passing by the cell.

Transmembrane currents were first calculated following standard 1-D cable theory (Rall, 1977), assuming that the extracellular potential was 0. The currents from each compartment were calculated using the NEURON simulation of Mainen and Sejnowski (1996) (we used their source code directly, obtaining it from `http://www.cnl.salk.edu/~zach/patdemo.html`). In the original model, the neuron was activated by an electrode in the soma. We removed the electrode and scattered synaptic input uniformly throughout the dendrites to provide input. We used the same approximation as Bernander *et al.* (1991): synapses were not explicitly modeled, but the leak resistance and reversal potential was changed to reflect the time-averaged synaptic conductance. A synaptic conductance of 0.2 times the leak conductance and a reversal potential of 0 mV in every compartment supplied enough current to make the cell fire after 35 ms. The intracellular resistivity R_i was 150 Ω cm. At specified times, the total current (capacitive + ionic) in each segment was recorded. The action potential was sampled at 0.01 ms during its steep rising phase, and at larger intervals elsewhere; the time step was 0.01 ms throughout.

Given these computed currents, the extracellular potential was calculated according to standard volume conductor theory (Stevens, 1966; Malmivuo and Plonsey, 1995). As in all previous theoretical studies of extracellular potential, we did not explicitly model all the elements in the space surrounding the cell. Instead, the local potential is replaced by its average over a small volume, and the medium is treated as an homogeneous isotroptic dielectric. Local geometrical irregularities will cause variations of extracellular potential on a spatial scale of less than a micron. However, on distance scales of several microns, the homogenization approximation should give approximately correct results. None of the results of this paper will be critically affected by the irregularities of the local microstructure. We also did not take into account any glial sheath, since cortical pyramidal cells, unlike many other kinds of cells in the nervous system, do not posess such a sheath (Peters *et al.*, 1991). The extracellular medium has a bulk resistivity of somewhere between 200 and 400 Ω cm and negligible reactance for the relevant temporal frequencies (Ranck, 1963; see also references in Plonsey, 1969). We used a value of extracellular conductivity of $\sigma_e = 1/330$ Ω cm. The potential and field amplitudes are proportional to $1/\sigma_e$ so the effect of a change in σ_e is easy to calculate.

We assumed that the previously calculated transmembrane currents will not be affected much by the small changes in extracellular potential. The extracellular potentials are in most places less than 1 mV, and it is difficult to see how these could possibly have a significant effect on the transmembrane currents. Larger potentials of $3-4$ mV occur very briefly and only near the axon initial segment. Depending on the transmembrane potential, extracellular potentials of this size could cause noticeable effects. However, the $3-4$ mV shifts occur when the membrane potential is about 0 mV (not shown). In this voltage range, the sodium channel is not sensitive to small voltage shifts. A 3 mV shift in the potential when it is near 0 mV changes m_∞^3 for the sodium channel in our model by less than 0.05 (with even less of an effect on τ_m or h_∞ or τ_h) and has only a 5% effect on the driving force. Therefore neglecting the effect of the extracellular potentials induced by a cell on its own transmembrane currents will have only a small effect on the time course and magnitude of the calculated currents. Other factors such as unknown

channel distributions will be more significant. Our goal is not to simulate the extracellular field exactly, but to provide an approximate solution to address more qualitative issues. Therefore we did not attempt to refine our estimate of the transmembrane currents after computing the extracellular potentials.

The electric potential in the extracellular space is governed by Laplace's equation,

$$\nabla \cdot (\sigma_e \nabla \phi) = 0 \tag{1}$$

where σ_e is the bulk conductivity tensor. At the boundaries, $\sigma_e \nabla \phi = \mathbf{J_m}$, where $\mathbf{J_m}$ is the transmembrane current density. For a single point source in an unbounded isotropic volume conductor, the solution is given by an analog of Coulomb's law,

$$\phi = \frac{i}{4\pi\sigma_e r}, \tag{2}$$

where r is the distance from the point source and i is current from the point source. A cable can be treated to a good approximation as a line of point sources (the *line source model*). The extracellular potential was computed as the sum of the potentials from all the points on the dendrites. Each dendrite was broken up into straight cylinders, one cylinder between each point recorded in the reconstruction (there were may more cylinders than there were segments in the 1-D NEURON model; the current from a given segment was assumed to be uniformly distributed across all cylinders composing the segment). The soma was treated as a sphere. For more details, see Holt (1998), appendix C.

Since extracellular potentials are computed very close to the membranes, it is reasonable to ask whether a model that treats a cable with finite diameter as a line with zero width is dependable close to the cable membrane. We compared the approximate solution from the line-source model with the solution of equation 1 for an infinitely long cylinder with a finite radius (the solution by separation of variables and eigenfunction expansion is straightforward; details can be found in Holt, 1998, appendix C). The line and cylinder source models were compared for an infinite cable of diameter 1 μm emitting a current over a 10 μm segment. Figure 1 shows the extracellular potential along the line $r = a$, i.e., at the neural membrane. The results are virtually indistinguishable; the line source model is definitely sufficiently accurate for computation, even close to the membranes. Using different simulations, others have also found the line source model to be very accurate (Rosenfalck, 1969, appendix 1; Trayanova and Henriquez, 1991).

The effect of the extracellular potential on a cable passing through the region was computed using the formalism in section 4. The equations were discretized and the resulting tridiagonal system solved using standard numerical techniques.

3 Extracellular potential around a simulated cell

We used a previously published model of a layer V, adult cat neocortical cell (Mainen and Sejnowski, 1996) without modification except that current injection through an electrode was replaced by time-invariant synaptic input (section 2). The morphology of the cell was

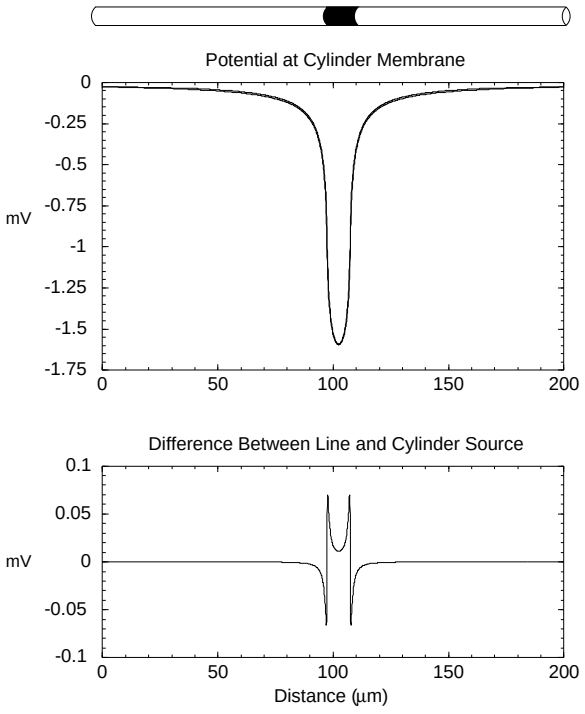

Figure 1: Justification of the line-source approximation for computation of extracellular potential near membranes. A long cable with a diameter of 1 μm has a 10 μm segment that emits current (dark region of cable). Extracellular potential was computed as a function of position along the cable at the membrane using either the line-source approximation (treating the cable as a line of zero width), or directly from equation 1 taking into account the finite diameter of the cable. *Top:* Potential at the membrane for the two methods. There are actually two lines on the figure; the results are almost indistinguishable. *Bottom:* The difference between calculated potential from the line source method and cylinder source method. Note the different scale on the y axis.

obtained using HRP during the course of *in vivo* experments in the visual cortex of an adult cat (Douglas *et al.*, 1991). This model was designed to replicate the results of Stuart and Sakmann (1994), in particular that action potentials initiated in the soma or axon even when current was injected into the dendrites. The cell has a very high density of sodium channels in the axon hillock and initial segment, and a low density in the soma and dendrites. Potassium currents (delayed rectifier, M-current, and calcium-dependent) and a calcium current are also present in the soma and dendrites. We could equally well have used the model of Rapp *et al.* (1996) except that it does not include repolarization currents.

Sample voltage traces are shown in figure 2. The action potential initiates approximately simultaneously in the distal part of the initial segment and the first node of Ranvier. It then propagates up the initial segment (not shown), slowing down considerably in the axon hillock because of the load of the soma and the dendrites (for the locations of these parts of the neuron, see the legend to figure 3).

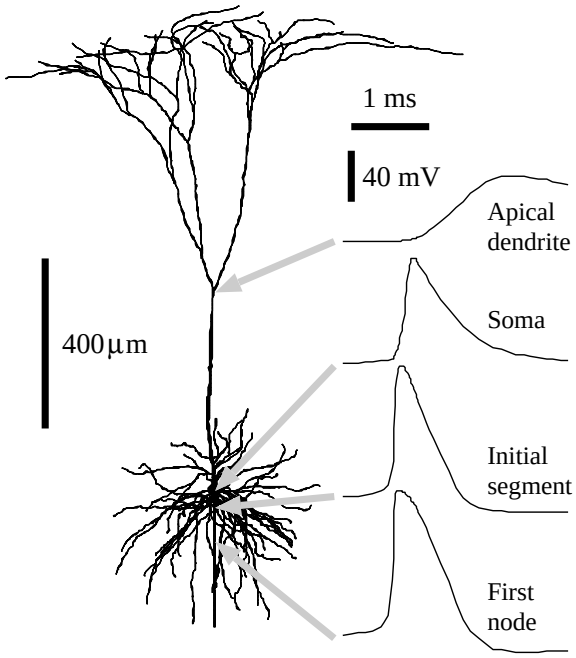

Figure 2: Intracellular voltages at several points in the simulated cell. Each trace is 3 ms long. The spike begins in the initial segment/first node and propagates into the soma and up the dendrites.

Using standard volume conductor theory, field potentials were computed from the compartmental model (figure 3 and figure 4). It is difficult to account for every detail of the field potential, but most of the obvious features can be understood. First consider the largest potentials, which occur near the axon hillock and initial segment. This area of the neuron has an extremely high density of sodium channels in the model (maximum conductance if all are open is 30,000 pS/μm^2, in comparison with 20 pS/μm^2 in the soma and dendrites). The inward currents are large because current through the axon hillock is what depolarizes the soma and proximal dendrites.

The initial negativity in the extracellular potential (called "A spike" by Terzuolo and

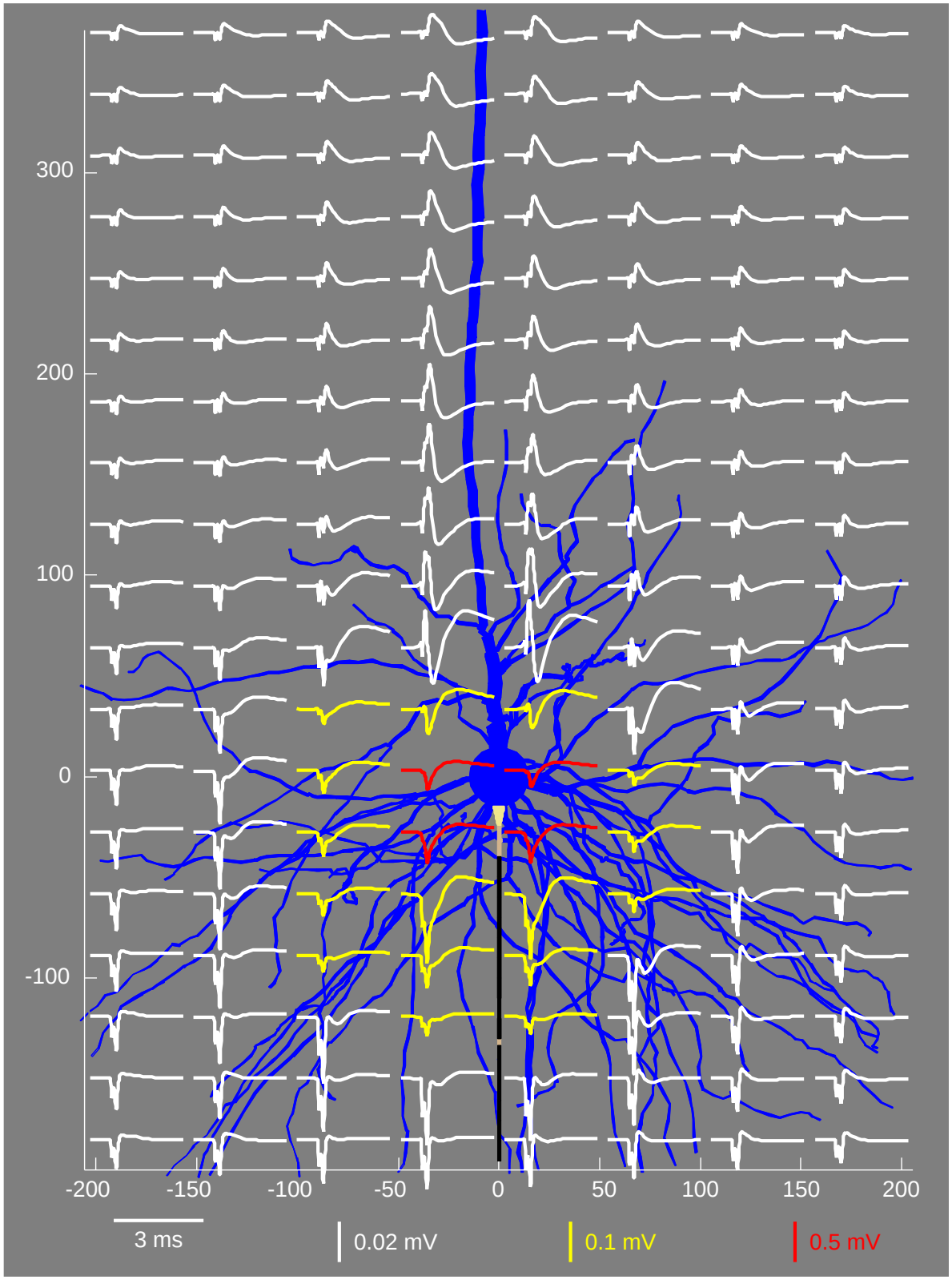

Figure 3: caption on page 12.

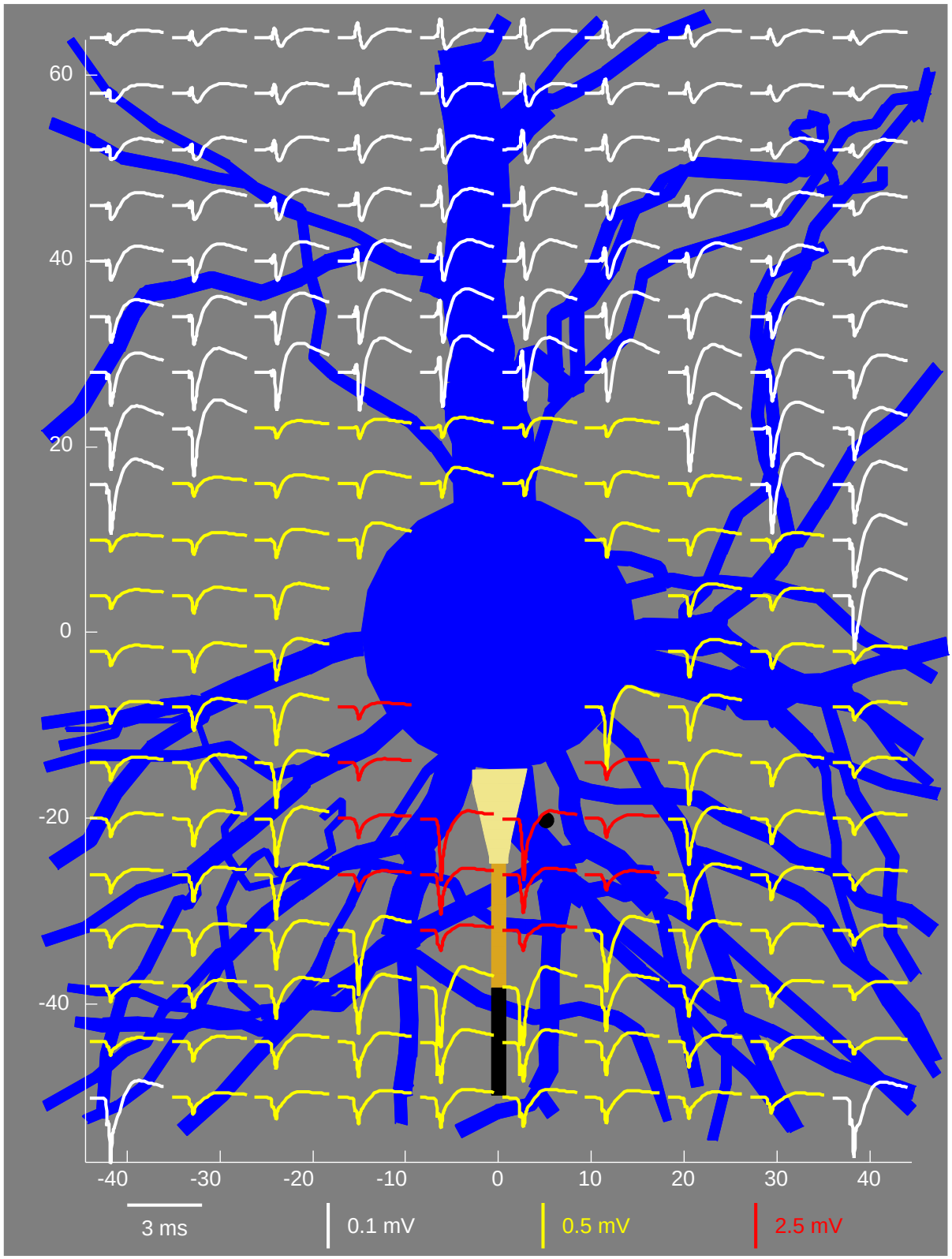

Figure 4: caption on page 12.

Figure 3: Field potentials in a plane around the simulated layer V cortical pyramidal cell. x and y axes are in units of μm. Each trace is the potential as a function of time at a point located at the center of the trace. Note the different voltage scales indicated by the different colors of traces. The superimposed neuron is a projection of the three dimensional shape onto the plane; many of the dendrites shown are above or beneath the plane of the figure. However, both the soma and the axon are in the plane of the figure. The axon hillock is marked in light tan; the initial segment and the first node of Ranvier are marked in darker tan; myelin is shown in black. Closer than 20 μm to the axon hillock, field potentials are much larger than shown here (see figure 4 for closeup). The soma is at $(0, 0)$, and the axon descends straight below it. The apical dendritic trunk is slightly to the left of $x = 0$ and goes up approximately straight, so the larger potentials at the top center are from the apical dendrite. The field potentials look roughly similar in slices at other angles through the volume, so only this slice is shown.

Figure 4: Field potentials near the soma of the simulated layer V cortical pyramidal cell. The peak field potential is slightly over -5 mV and occurs next to the axon hillock (light tan). Note that the peak amplitude on this graph is much higher than in figure 3 because the traces are closer to the axon initial segment. The black spot near the axon hillock is the location of the cable of figures 8 and 9.

Araki, 1961 in analogy with the A and B spikes in the transmembrane potential) is due to currents in the distal initial segment, since it occurs at the same time as the maximum current from the distal initial segment (see figure 5). Because of charge conservation, current flowing in through the initial segment must flow out somewhere in the cell; in fact, there is an initial positivity near the apical dendrite (figure 3) because the potential from the local outward current there was larger than the potential from the inward current at the initial segment. A sign reversal is not observed in the basal tree because it is approximately a closed field.

A second negativity (the "B spike") in the field potential is due to the currents in the axon hillock, especially the proximal part (figure 5). This negativity is larger because the total current into the hillock is larger than into the initial segment. In fact, the field potential can be as large as -5 mV within a few microns of the hillock. Again, this reverses in sign in the apical dendrite because of current outflow there.

In the model, the action potential propagates up the apical tree[1], but dV_m/dt is very small because of the much lower sodium channel density. The field potentials are therefore extremely small (sometimes less than 10 μV) and are difficult to observe directly.

There are several important features of the extracellular action potential for ephaptic interaction. First, as noted above, it is much larger than the extracellular potential expected around axons under most conditions. Second, it is more confined in space than fields from axons (figure 6A). For an axon in a sheath, for example, it is known that the

[1] A movie of this can be seen at `http://www.klab.caltech.edu/~holt/thesis/`.

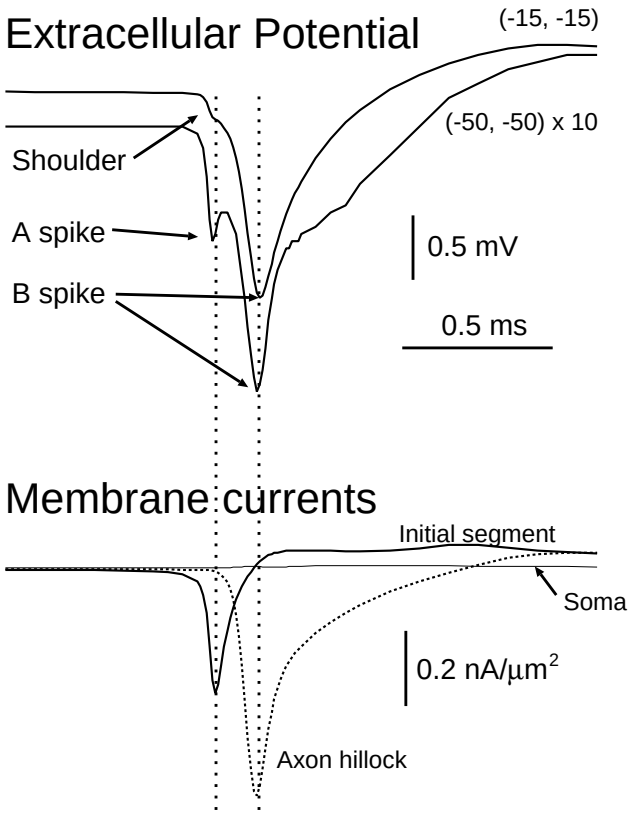

Figure 5: A comparison of the field potential and transmembrane currents. The first negativity in the field potential corresponds to the maximum current from the distal initial segment. The second negativity corresponds to the maximum current from the proximal axon hillock. The current trace labelled "soma" is the current through the soma on the same scale; in this model, somatic currents were far smaller than hillock/initial segment currents so the line is almost flat.

extracellular potential $\phi \propto -V_m$ (Clark and Plonsey, 1968; Rosenfalck, 1969; Stein and Pearson, 1971), so the field may be spread out over a mm or more depending on the speed of propagation (figure 6A). In contrast, the extracellular field has a large amplitude over only a small region (50 μm for this particular model, as shown in figure 6B; sometimes over 100 μm measured experimentally).

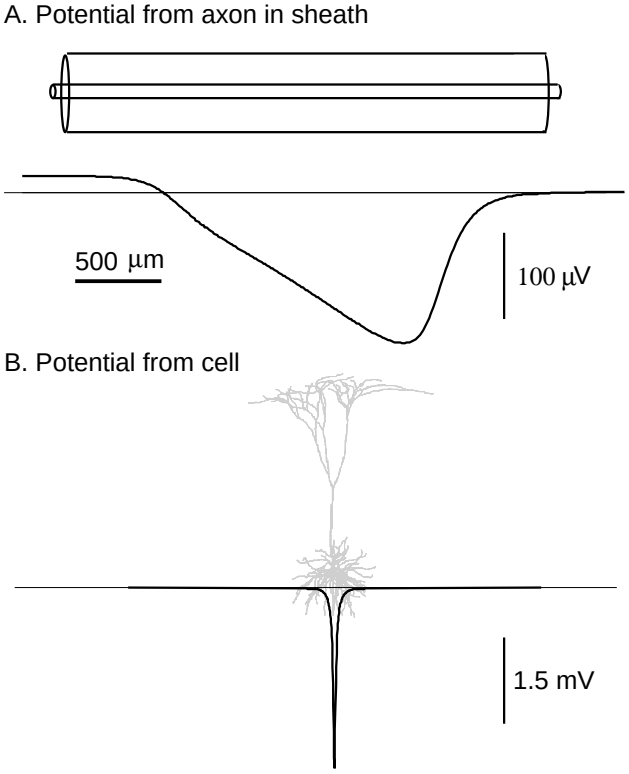

Figure 6: A comparison of the extracellular potential produced by a long axon (**A**) and a pyramidal cell body (**B**). The axon had a diameter of 1 μm and channels as given by the usual Hodgkin–Huxley equations. The extracellular potential around an axon in a sheath is simply $V_m \propto -V_e$; the amplitude is inversely proportional to the square of the sheath diameter, and is expected to be tens to hundreds of microvolts at most. The potential from the cell was computed along a line perpendicular to the plane of figure 3 and intersected it at $(5, -20)$ (near the axon hillock). Voltage scale is arbitrary in A, since the voltage depends strongly on the radius of the sheath.

4 Effect of extracellular potential on neural elements

Consider a straight passive unmyelinated cable with a varying extracellular electric potential V_e, as shown in figure 7. (V_e is equal to the extracellular potential ϕ at the membrane surface. If the extracellular potential ϕ varies significantly around the perimeter of the membrane, then V_e is the average value of ϕ.) Summing the currents into the junction and taking the limit as the differentials approach 0 gives (Clark and Plonsey, 1971; Plonsey and Barr, 1995)

$$\begin{aligned} c_m \frac{\partial V_m}{\partial t} + g_m V_m &= \frac{\partial}{\partial z} \frac{1}{r_i} \frac{\partial V_i}{\partial z} \\ &= \frac{\partial}{\partial z} \frac{1}{r_i} \left(\frac{\partial V_m}{\partial z} + \frac{\partial V_e}{\partial z} \right) \end{aligned} \tag{3}$$

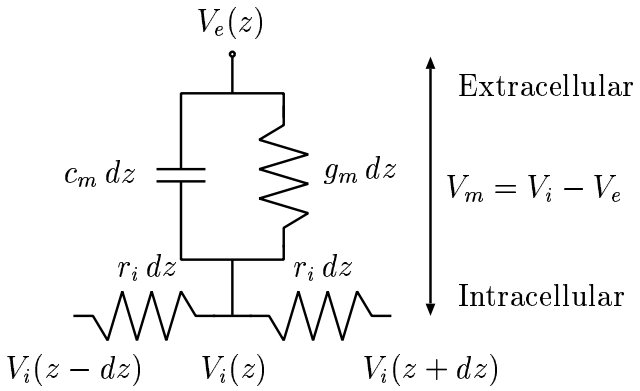

Figure 7: Circuit for computing the effect of extracellular potentials.

---

since $V_m = V_i - V_e$. With the usual definitions $\tau = c_m/g_m$ and $\lambda^2 = 1/r_i g_m$, and assuming r_i is constant, this becomes

$$\tau \frac{\partial V_m}{\partial t} + V_m = \lambda^2 \left(\frac{\partial^2 V_m}{\partial z^2} + \frac{\partial^2 V_e}{\partial z^2} \right). \tag{4}$$

This is the standard cable equation except for the last term. It is possible to interpret equation 4 as the normal cable equation if the effect of the extracellular potential is thought of as a fictitious distributed current (the *ephaptic current*) with a magnitude of

$$i_{eph} = \frac{\partial}{\partial z} \frac{1}{r_i} \frac{\partial V_e}{\partial z} \tag{5}$$

per unit length.

For an intuitive understanding, it is helpful to consider the Fourier transform of equation 4 in both space (k) and time (ω):

$$i\omega\tau \hat{V}_m + \hat{V}_m = -k^2\lambda^2 \hat{V}_m - k^2\lambda^2 \hat{V}_e \tag{6}$$

or

$$\hat{V}_m = \frac{-k^2\lambda^2}{1 + i\omega\tau + k^2\lambda^2} \hat{V}_e. \tag{7}$$

Clearly the biggest that $|\hat{V}_m|$ can ever be is $|\hat{V}_e|$, and that occurs for large $k^2\lambda^2$. This suggests that the largest $V_m(z)$ can be is $-V_e(z)$, which occurs when $V_i(z)$ is approximately constant. In the extreme case, if the intracellular medium is a perfect conductor (e.g., the cable is a metal wire), then V_i will not change at all. V_i will be almost constant if the intracellular resistance between the point at z and another point where V_e is substantially different is small.

This upper bound is not reached in practice for two axons in a bundle. Instead, the term $i\omega\tau$ in the denominator of equation 7 dominates over the relevant frequency range, and the main ephaptic effect is on the time derivative of V_m (Clark and Plonsey, 1971).

The potential around cells is much more confined than around axons, and therefore $k\lambda$ is much bigger. For example, from figure 3, the dominant spatial frequency in the action potential is somewhere around $k = 2\pi/100/\mu$m and the dominant temporal frequency is $\omega = 2\pi/0.30/$ms. If an axon with a diameter of 1 μm and the same passive parameters as the axons in Manor *et al.* (1991) at rest ($\tau = 1.1$ ms, $\lambda = 220$ μm) passes by this cell body, $k^2\lambda^2 \approx 190$ and $\omega\tau \approx 20$. Unlike interaction between pairs of axons, near a cell body $k^2\lambda^2 \gg \omega\tau$. Because of the much shorter distances involved, the intracellular medium acts as a good conductor, so V_i is approximately unchanged. As a result, we would expect that $V_m \approx -V_e$ and has the same time course as V_e.

Despite the crudity of this analysis, it is not a bad predictor of the transmembrane potential. The actual transmembrane potential is shown in figure 8. In fact, V_m is almost equal to $-V_e$, especially near the cell body where V_e is changing rapidly with position.

Kinks or bifurcations in the cable give rise to higher spatial frequencies in V_e, because the direction of the cable changes discontinuously. This would make V_m even closer to $-V_e$. However, in the example considered here, V_m is already almost equal to V_e, so kinks are not expected to make a large difference. For potentials spread out more in space, these geometrical inhomogeneities could make a significant difference. For completeness, a method for computation of the effects of kinks, bends, bifurcations, and terminations is described in the appendix to this paper.

Ephaptic interaction can be characterized by localized current injection (equation 5), just as synapses can. However, this example shows that ephapses have somewhat different properties from synapses. Because the ephaptic current depends on the second derivative of the extracellular potential, a peak in the extracellular potential produces an ephaptic current which is depolarizing at the peak and a hyperpolarization that flanks the peak (see the currents (*dashed lines*) in figure 8). In fact, the total ephaptic current into an cable is given by

$$\begin{aligned}\int_{-\infty}^{\infty} i_{eph}(t)\,dz &= \int_{-\infty}^{\infty} \frac{1}{r_i}\frac{\partial^2 V_e(t)}{\partial z^2}\,dz \\ &= \frac{1}{r_i}\left(\lim_{z\to\infty}\frac{\partial V_e(t)}{\partial z} - \lim_{z\to-\infty}\frac{\partial V_e(t)}{\partial z}\right) \\ &= 0.\end{aligned}$$

As a result, the transmembrane potential is more localized and does not spread in the same way as a point current source injection would.

The Fourier analysis also predicts what the effect of parameter variations is on the induced potential. Since $k^2\lambda^2 \gg \omega\tau$, changing $\tau = c_m/g_m$ by changing the capacitance within reasonable limits should have little effect on the result (figure 9A), so myelination will not significantly affect interaction. Also changing $\lambda = \sqrt{\sigma_i d/4g_m}$ by changing the intracellular resistivity (figure 9B) or the cable diameter d (figure 9C) within physiological limits has little effect because $k^2\lambda^2$ appears in both the numerator and the denominator. Changing the membrane conductance g_m has the same effect on both $k^2\lambda^2$ and $\omega\tau$ and has little effect on the result as long as $\omega\tau + k^2\lambda^2 \gg 1$ (figure 9D).

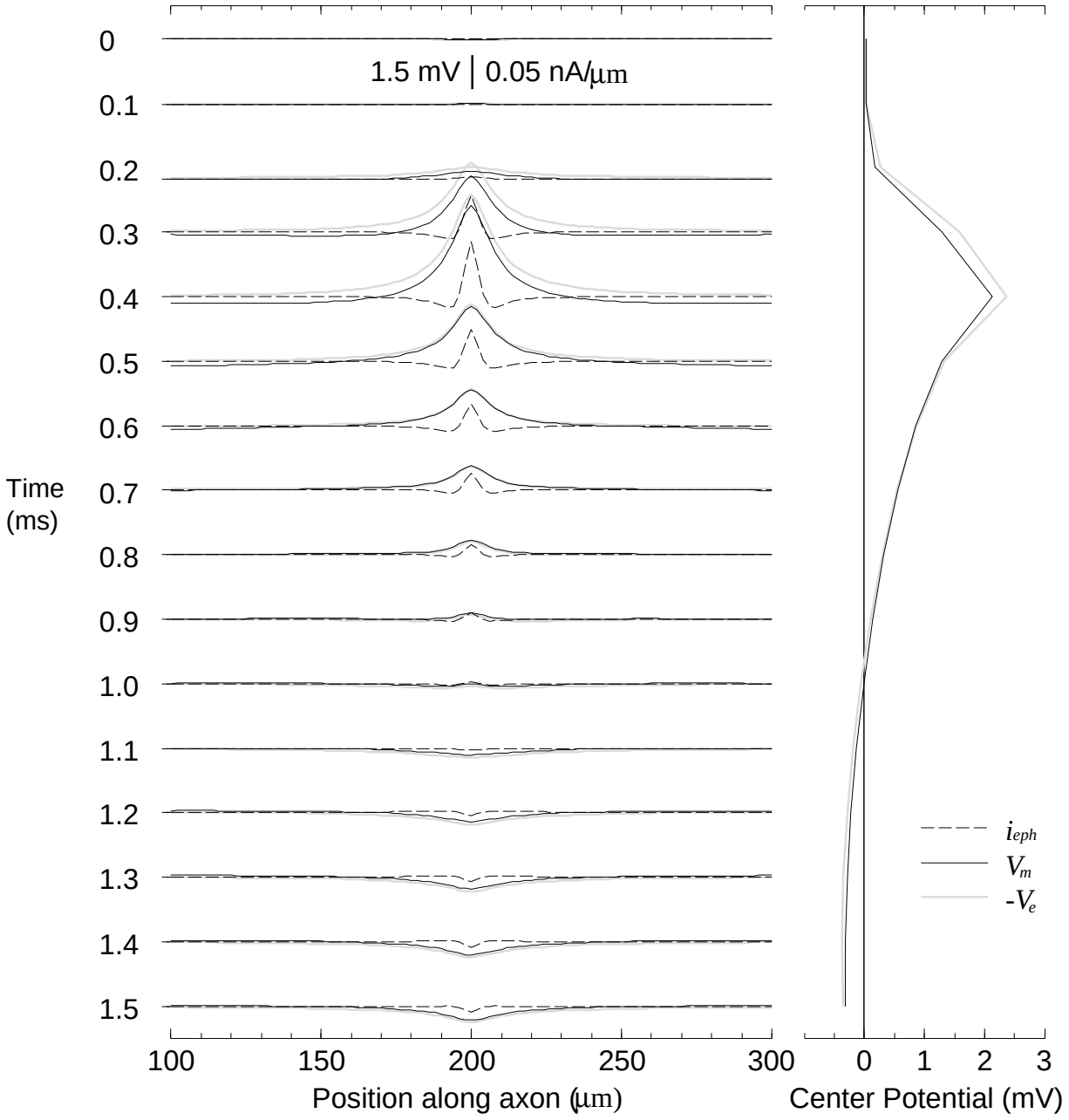

Figure 8: The membrane potential of a long straight passive cable located about 2 μm from the axon hillock of the simulated layer V pyramidal cell. *Left:* Extracellular potential, transmembrane potential induced in the cable, and the ephaptic current are shown as a function of position for several different times during an action potential in the pyramidal cell. *Right:* Extracellular and transmembrane potential at the point where the axon passes closest to the cell body. This cable was perpendicular to the plane of figure 3 and intersected it at $(5, -20)$ (marked by the black dot on figure 4 several microns from the axon hillock). Parameters: $d = 1$ μm, $c_m = 0.8$ μF/cm^2, $g_m = 1/1400$ Ω cm^2 (same as the axon in Manor *et al.*, 1991).

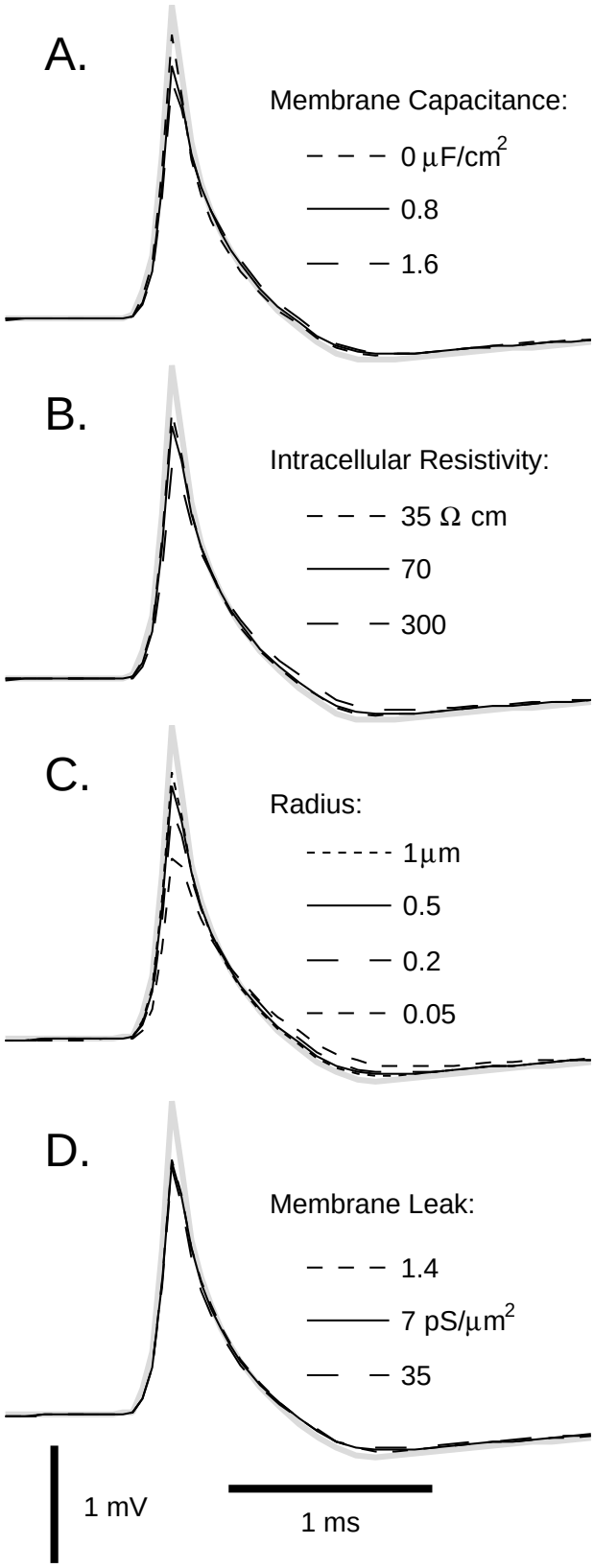

Figure 9: Effect of varying cable parameters on the transmembrane voltage induced by the extracellular spike of the pyramidal cell shown in figures 3 and 4. Only the voltage at the center of the cable (the peak voltage; position 200 μm in figure 8 left) is shown. In each plot, $-V_e$ is shown in grey and the induced potential V_m is shown in solid black lines. **A**: Variations in capacitance c_m, affecting only τ. **B**: Variations in intracellular resistivity, affecting only λ. **C**: Variations in the radius of the axon, which affects only λ. **D**: Variations in the membrane conductivity, which affects both λ^2 and τ proportionately. In all cases, there is little change in the induced transmembrane potential within physiologically reasonable limits.

Similar results are to be expected from changing parameters in only a small region of the cable. This is difficult to analyze quantitatively, but the same qualitative considerations hold. Since the intracellular potential is approximately constant, the transmembrane potential will be approximately the negative of the extracellular potential. Local changes in conductivity or diameter will not significantly affect this relationship, and thus do not have a large effect on the magnitude of the induced voltage.

The only parameter that has a large effect on the magnitude of ephaptic voltage transients is the location of the cable. The magnitude of the extracellular electrical field decreases sharply with distance; more than 20 μm away from the axon hillock, the peak extracellular potential amplitude has dropped to less than 1 mV in this simulation, and the induced transmembrane voltages also drop by the same amount.

In these simulations, the cable runs perpendicular to the dendritic axis of the cell. However, cables running parallel to the apical dendrites would feel similar extracellular fields, provided they pass close enough to the axon hillock, because the falloff of extracellular potential with distance is approximately independent of direction (not shown) when the potential is greater than 1 mV. (Below 1 mV the potential falloff is anisotropic but such such potential magnitudes are unlikely to be important for interaction.)

5 Discussion

Using standard volume conductor theory, we computed the approximate extracellular potential that would be produced by a spiking pyramidal cell in a previously published compartmental model simulation (Mainen and Sejnowski, 1996). This model was chosen because its spikes initiate in the axon (Mainen *et al.*, 1995). Proper location of spiking currents is important for computing the extracellular potential, because potentials are much larger near regions of large current densities (figure 4). However, we believe that our results—in particular as they pertain to ephaptic interactions—hold true for many neuronal geometries and distributions of membrane currents within physiological bounds.

5.1 Extracellular potential waveforms

The simulated extracellular action potentials (figures 3 and 4) resemble a number of previously published estimates for several different kinds of neurons (e.g., Fatt, 1957; Freygang, 1958; Freygang and Frank, 1959; Nelson and Frank, 1964; Sperti *et al.*, 1967; Rosenthal, 1972), both in magnitude and in shape. In our simulations, within a radius 10–20 micrometers of the axon hillock, the extracellular potentials can be over 1 mV in amplitude. They reach a peak of about 5 mV at the membrane of the axon hillock. We used an extracellular resistivity of 330 Ω cm; the extracellular potential is roughly proportional to the resistivity, so the effects of different resistivities are easy to estimate.

The potentials have up to two peaks far from the cell body, and a peak with a shoulder near the cell body (figure 5). The amplitude of the first peak is quite small in most places, and might not be observable in many recordings. A peak with a shoulder would

be observable near the axon initial segment. In fact, often a shoulder on the waveform is seen near the soma of a variety of neurons, including CA1 pyramidal cells (Sperti *et al.*, 1967; Buzsáki *et al.*, 1996), possibly pyramidal tract neurons (figure 1 of Rosenthal, 1972), and motoneurons (Fatt, 1957; Terzuolo and Araki, 1961; Nelson and Frank, 1964). In some published traces, two separate peaks rather than just a shoulder can sometimes be discerned (e.g., Fatt, 1957).

By direct comparison of intracellular with extracellular voltage, the first peak (the extracellular A spike) has classically been attributed to the axon hillock/initial segment, and the second (the extracellular B spike) to the soma and possibly proximal dendrites (Terzuolo and Araki, 1961). In the model here, however, both the A and the B spike are from currents in the axon; the A spike comes from the initial segment, and the B spike comes primarily from the axon hillock. This probably could not be discerned experimentally because the potential in the soma very closely follows the potential in the axon hillock, and the transmembrane currents were not measured directly.

There is some disagreement about whether strong currents exist in the axon hillock and initial segment. The classical model of spike initiation developed for motoneurons is that the axon hillock/initial segment has a very high density of sodium channels, causing action potentials to initiate there first (Fuortes *et al.*, 1957; Coombs *et al.*, 1957a, 1957b) and then propagate into the soma and dendrites. A similar idea has recently been proposed for neocortex (Mainen *et al.*, 1995; Rapp *et al.*, 1996). On the other hand, recent measurements in hippocampal cells (Colbert and Johnston, 1996) suggest that there is a low density of sodium channels in the axon hillock and initial segment, and that the large currents must be located at the first node of Ranvier. Measuring the extracellular potentials in a slice may be a simple way to determine where the large currents are.

Extracellular potentials can also be used to infer a number of other properties of the system. For example, 50 years before intracellular dendritic measurement became routine, Lorente de Nó (1947) was able to conclude from extracellular potentials that branch point failure occurs in propagation of action potentials into the dendritic tree (see also Buzsáki *et al.*, 1996 for a similar modern inference). In general, studies of extracellular potential may provide valuable clues to the distributions of currents in a neuron, especially when it is possible to test interpretations of the extracellular potential with a compartmental model and neurons with known geometries. Current-source density analysis uses approximate anatomical information about populations of neurons to infer synaptic currents (e.g., see Mitzdorf, 1985), but additional information is available in the spatial pattern of potential from a single neuron which is often washed out by population-based analyses.

5.2 Effect of extracellular potential on other neurons

The effect of extracellular potential on neural elements has been studied extensively to understand the effect of stimulating electrodes (e.g., Ranck, 1975; MacNeal, 1976; Tranchina and Nicholson, 1986; Chan and Nicholson, 1986). Similarly, influence of one axon on another in a fiber tract is well understood (e.g., Clark and Plonsey, 1970, 1971; Markin, 1970a, 1970b, 1973a; Barr and Plonsey, 1992, among many other studies). We find that ephaptic

interactions between the cell body of a neuron and a nearby axon or dendrite have qualitatively different properties from these cases, because the potential fields are qualitatively different. In the case of two interacting axons, the temporal derivative of the membrane potential is roughly proportional to the extracellular potential spatial differences (Clark and Plonsey, 1971). However, for a cable passing by a cell body, the transmembrane potential (not its derivative) is approximately equal to the negative of the extracellular potential. The extracellular potential around a cell body is much more spatially confined than the extracellular potential along an axon (figure 6). As a result, the relevant spatial distances along the cable are much shorter, and the intracellular resistance is much less. As a result, the interior of the cable is approximately isopotential, so the transmembrane potential has almost the same magnitude as the extracellular potential.

Ephaptic interactions near cell bodies can give rise to larger depolarizations than typical excitatory chemical synapses between pyramidal cells. Unlike chemical synapses, however, the effect does not spread electrotonically. As a result, ephaptic depolarizations will have no lasting effect unless there are active channels at the location of the ephaptic depolarization. This is different from ordinary synapses, because small synaptic currents from many locations can sum together to form a substantial depolarization at a site quite distant from the synapses.

Since the ephaptic depolarizations are localized and are only a few mV at most, they will have an effect only on structures already close to threshold. For example, there is some evidence that action potential propagation can fail at branch points in the axon (Swadlow *et al.*, 1980; Debanne *et al.*, 1997) or dendrites (Lorente de Nó, 1947; Buzsáki *et al.*, 1996; Hoffman *et al.*, 1997). In this case, the potential in each of the branches would be close to threshold and a simultaneous extracellular action potential might be enough to cause the action potential to invade the branch.

Can ephaptic interactions from simultaneously active neurons lead to larger effects? Extracellular potentials from two neurons should approximately superpose, unless the changes in membrane conductance change the bulk conductance of the volume significantly, or the potential changes become large enough to affect the spiking currents noticeably. However, since extracellular spike waveforms are brief and have positive as well as negative regions, spikes must be aligned to significantly less than a ms if they are to add constructively to form a larger potential. (This is one reason why spiking activity is thought to be a relatively minor component of bulk field potentials in EEG and current source-density analysis; e.g., see Mitzdorf, 1985.) It is unlikely that such precise synchrony is common.

Ephaptic interactions are more difficult to modify than chemical synapses once a neurite is grown, because the magnitude of the depolarization is roughly independent of the cable properties of the post-ephaptic membrane (figure 9). If ephaptic effects are to subserve some function, then it would be reasonable to expect that growth cones are directed by the electric fields set up by cell spiking activity. Growth cones are indeed often affected by electrical fields, both steady state (McCaig, 1988; McCaig and Zhao, 1997) and pulsed fields (Patel and Poo, 1984). Minimum peak field amplitudes for growth cone direction could be as low as 6 mV/mm, which is considerably smaller than the peak field amplitudes calculated above, so long as the pulse frequency is high enough. If spiking activity during

development has any significant effect on growth cones, it usually would tend to guide neurites toward the cell bodies of spiking cells.

It has been sporadically suggested that dendritic bundles might be an anatomical substrate for ephaptic coupling (e.g., see Roney *et al.*, 1979; Jefferys, 1995 and references therein). However, unless extracellular conductivity within the bundles is dramatically different from the measured bulk conductivities, ephaptic coupling due to spikes propagating up the dendritic tree will be negligible since the extracellular potentials will be only tens of microvolts except near the axon hillock. Coupling in bundles based on slow extracellular potentials (e.g., summed synaptic currents from many neurons) is possible but the physics of coupling is different due to the different temporal and spatial scales.

Ephaptic interactions with magnitudes of several mV are just on the verge of being significant. The magnitude is approximately proportional to the extracellular resistivity; if this were much higher, ephaptic effects would be much more widespread in the central nervous system. Some cross-talk may occasionally be useful for computation, but widespread crosstalk would probably be damaging. Extracellular resistivity is controlled primarily by the size and tortuosity of the extracellular medium. It is therefore possible that the need to limit noise from cross-talk is what determines the minimum spacing between neural elements.

Acknowledgements

We thank David Kewley and James Bower for helpful discussions about electrical potentials and ephaptic interactions and Zachary Mainen and Terrence Sejnowski for making their model of a cortical pyramidal cell available on the web. The research reported here was supported by the Sloan Center for Theoretical Neuroscience at Caltech as well as by the NIMH and NSF.

References

Arvanitaki, A. 1942. Effects evoked in an axon by the activity of a contiguous one. *J. Neurophysiol.* 5:89–108.

Barr, R. C., and Plonsey, R. 1992. Electrophysiological interaction through the interstitial space between adjacent unmyelinated parallel fibers. *Biophys. J.* 61:1164–1175.

Bernander, Ö., Douglas, R., Martin, K., and Koch, C. 1991. Synaptic background activity determines spatio-temporal integration in single pyramidal cells. *Proc. Natl. Acad. Sci. USA* 88:1569–1573.

Bishop, G. H., and O'Leary, J. L. 1942. The polarity of potentials recorded from the superior colliculus. *J. Cell. Comp. Physiol.* 19:289–300.

Bullock, T. H. 1965. Comparative neurology of transmission. In: *Structure and Function in the Nervous Systems of Invertebrates. Vol. I.*. Bullock, T. H., Horridge, G. A., eds., pp. 181-251. W. H. Freeman.

Bullock, T. H. 1997. Signals and signs in the nervous system: The dynamic anatomy of electrical activity is probably information-rich. *Proc. Natl. Acad. Sci. USA* 94:1–6.

Buzsáki, G. , Penttonen, M., Nádasdy, Z. , and Bragin, A. 1996. Pattern and inhibition-dependent invasion of pyramidal cell dendrites by fast spikes in the hippocampus *in vitro*. *Proc. Natl. Acad. Sci. USA* 93:9921–9925.

Chan, C. Y., and Nicholson, C. 1986. Modulation by applied electric fields of purkinje and stellate cell activity in the isolated turtle cerebellum. *J. Physiol.* 371:89–114.

Clark, J., and Plonsey, R. 1968. The extracellular potential field of the single active nerve fiber in a volume conductor. *Biophys. J.* 8:842–864.

Clark, J. W., and Plonsey, R. 1970. A mathematical study of nerve fiber interaction. *Biophys. J.* 10:937–957.

Clark, J. W., and Plonsey, R. 1971. Fiber interaction in a nerve trunk. *Biophys. J.* 11:281–294.

Colbert, C. M., and Johnston, D. 1996. Axonal action-potential initiation and Na^+ channel densities in the soma and axon initial segment of subicular neurons. *J. Neurosci.* 16:6676–6686.

Coombs, J. S., Curtis, D. R., and Eccles, J. C. 1957a. The interpretation of spike potentials of motoneurons. *J. Physiol.* 139:198–231.

Coombs, J. S., Curtis, D. R., and Eccles, J. C. 1957b. The generation of impulses in motoneurons. *J. Physiol.* 139:232–249.

Dalkara, T., Krnjević, K., Ropert, N., and Yim, C. Y. 1986. Chemical modulation of ephaptic activation of CA3 hippocampal pyramids. *Neurosci.* 17:361–370.

Debanne, D., Guérineau, N. C., Gähwiler, B. H., and Thompson, S. M. 1997. Action-potential propagaion gated by an axonal I_A-like K^+ conductance in hippocampus. *Nature* 389:286–289.

Douglas, R. J., Martin, K. A. C., and Whitteridge, D. 1991. An intracellular analysis of the visual responses of neurones in cat visual cortex. *J. Physiol.* 440:659–696.

Eccles, J. C. 1964. *The Physiology of Synapses*. New York: Academic Press.

Faber, D. S., and Korn, H. 1989. Electrical field effects: Their relevance in central neural networks. *Physiol. Rev.* 69:821–863.

Fatt, P. 1957. Electric potentials occuring around a neurone during its antidromic activation. *J. Neurophysiol.* 20:27–60.

Freygang, W. H. 1958. An analysis of extracellular potentials from single neurons in the lateral geniculate nucleus of the cat. *J. Gen. Physiol.* 41:543–564.

Freygang, W. H., and Frank, K. 1959. Extracellular potentials from single spinal motoneurons. *J. Gen. Physiol.* 42:749–760.

Fuortes, M. G. F., Frank, K., and Becker, M. C. 1957. Steps in the production of motoneuron spikes. *J. Gen. Physiol.* 40:735–752.

Hoffman, D. A., Magee, J. C., Colbert, C. M., and Johnston, D. 1997. K^+ channel regulation of signal propagation in dendrites of hippocampal pyramidal neurons. *Nature* 387:869–875. Correction in Nature 390:199, 1997.

Holt, G. R. 1998. A critical reexamination of some assumptions and implications of cable theory in neurobiology. Ph. D. thesis, California Institute of Technology. Available

from `http://www.klab.caltech.edu/~holt/papers/thesis/`.

Hubbard, J. I., Llinás, R., and Quastel, D. M. J. 1969. *Electrophysiological Analysis of Synaptic Transmission.* Baltimore: Williams & Wilkins.

Jefferys, J. G. R. 1995. Nonsynaptic modulation of neuronal activity in the brain: Electric current and extracellular ions. *Physiol. Rev.* 75:689–723.

Katz, B., and Schmitt, O. H. 1942. A note on interaction between nerve fibers. *J. Physiol.* 100:369–371.

Kocsis, J. D., Ruiz, J. A., and Cummins, K. L. 1982. Modulation of axonal excitability mediated by surround electrical activity: An intra-axonal study. *Exp. Brain Res.* 47:151–153.

Korn, H., and Axelrad, H. 1980. Electrical inhibition of Purkinje cells in the cerebellum of the rat. *Proc. Natl. Acad. Sci. USA* 77:6244–6247.

Korn, H., and Faber, D. S. 1980. Electrical field effect interactions in the vertebrate brain. *Trends Neurosci.* 3:6–9.

Lorente de Nó, R. 1947. Action potential of the motoneurons of the hypoglossus nucleus. *J. Cell. Comp. Physiol.* 29:207–287.

MacNeal, D. R. 1976. Analysis of a model for excitation of myelinated nerve. *IEEE Trans. Biomed. Eng.* BME-33:329–337.

Mainen, Z. F., Joerges, J., Huguenard, J. R., and Sejnowski, T. J. 1995. A model of spike initiation in neocortical pyramidal neurons. *Neuron* 15:1427–1439.

Mainen, Z. F., and Sejnowski, T. J. 1996. Influence of dendritic structure on firing pattern in model neocortical neurons. *Nature* 382:363–366.

Malmivuo, J., and Plonsey, R. 1995. *Bioelectromagnetism: Principles and Applications of Bioelectric and Biomagnetic Fields.* Oxford University Press.

Manor, Y., Koch, C., and Segev, I. 1991. The effect of geometrical irregularities on propagation delay in axonal trees. *Biophys. J.* 60:1424–1437.

Markin, V. S. 1970a. Electrical interaction of parallel non-myelinated nerve fibers. I. Change in excitability of the adjacent fiber. *Biofizika* 15:120–128.

Markin, V. S. 1970b. Electrical interaction of parallel non-myelinated nerve fibers. II. Collective conduction of impulses. *Biofizika* 15:681–689.

Markin, V. S. 1973a. Electrical interaction of parallel non-myelinated nerve fibers. III. Interaction in bundles. *Biofizika* 18:314–321. Translated.

Markin, V. S. 1973b. Electrical interaction of parallel non-myelinated nerve fibers. IV. Role of anatomical inhomogeneities of nerve trunks. *Biofizika* 18:512–518. Translated.

McCaig, C. D. 1988. Nerve guidance: A role for bio-electric fields? *Prog. Neurobiol.* 30:449–468.

McCaig, C. D., and Zhao, M. 1997. Physiological electrical fields modify cell behaviour. *Bioessays* 19:819–826.

Mitzdorf, U. 1985. Current source-density method and application in cat cerebral cortex: Investigation of evoked potentials and EEG phenomena. *Physiol. Rev.* 65:37–100.

Nelson, P. G. 1966. Interaction between spinal motoneurons of the cat. *J. Neurophysiol.* 29:275–287.

Nelson, P. G., and Frank, K. 1964. Extracellular potential fields of single spinal motoneurons. *J. Neurophysiol.* 27:913–927.

Nicholson, C. 1995. Extracellular space as the pathway for neuron-glial cell interaction. In: *Neuroglia.* Kettenmann, H., Ransom, B. R., eds., pp. 387-397. Oxford University Press.

Patel, N. B., and Poo, M. M. 1984. Perturbation of the direction of neurite growth by pulsed and focal electric fields. *J. Neurosci.* 4:2939–2947.

Peters, A., Palay, S. L., and deF. Webster, H. 1991. *The Fine Structure of the Nervous System: The Neurons and Supporting Cells.* Philadelphia: W. B. Saunders Company.

Plonsey, R. 1969. *Bioelectric Phenomena.* New York: McGraw-Hill.

Plonsey, R., and Barr, R. C. 1995. Electric field stimulation of excitable tissue. *IEEE Trans. Biomed. Eng.* 42:329–336.

Rall, W. 1962. Electrophysiology of a dendritic neuron model. *Biophys. J.* 2:145–167.

Rall, W. 1977. Core conductor theory and cable properties of neurons. In: *The Nervous System, Vol. I: Cellular Biology of Neurons, Part 1.* Kandel, E. R., ed., pp. 39-97. Bethesda: American Physiological Society.

Ranck, J. B. 1963. Specific impedance of rabbit cerebral cortex. *Exp. Neurol.* 7:144–152.

Ranck, J. B. 1975. Which elements are excited in electrical stimulation of mammalian central nervous system: A review. *Brain Res.* 98:417–440.

Rapp, M., Yarom, Y., and Segev, I. 1996. Modeling back propagating action potential in weakly excitable dendrites of neocortical pyramidal cells. *Proc. Natl. Acad. Sci. USA* 93:11985–11990.

Roney, K. J., Scheibel, A. B., and Shaw, G. L. 1979. Dendritic bundles: Survey of anatomical experiments and physiological theories. *Brain Res. Rev.* 1:225–271.

Rosenfalck, P. 1969. Intra- and extracellular potential fields of active nerve and muscle fibers. *Acta Physiol. Scand. Suppl.* 321:1–168.

Rosenthal, F. 1972. Extracellular fields of single PT-neurons. *Brain Res.* 36:251–263.

Scott, A. C., and Luzader, S. D. 1979. Coupled solitary waves in neurophysics. *Physica Scripta* 20:395–401.

Snow, R. W., and Dudek, F. E. 1984. Electrical fields directly contribute to action potential synchronization during convulsant-induced epileptiform bursts. *Brain Res.* 323:114–118.

Sperti, L., Gessi, T., and Volta, F. 1967. Extracellular potential field of antidromically activated CA1 neurons. *Brain Res.* 3:343–361.

Stein, R. B., and Pearson, K. G. 1971. Predicted amplitude and form of action potentials recorded from unmyelinated nerve fibres. *J. Theor. Biol.* 32:539–558.

Stevens, C. F. 1966. *Neurophysiology: A Primer.* New York: John Wiley & Sons.

Stuart, G., and Sakmann, B. 1994. Active propagation of somatic action potentials into neocortical pyramidal cell dendrites. *Nature* 367:69–72.

Swadlow, H. A., Kocsis, J. D., and Waxman, S. G. 1980. Modulation of impulse conduction along the axonal tree. *Ann. Rev. Biophys. Bioeng.* 9:143–179.

Syková, E. 1997. The extracellular space in the CNS: Its regulation, volume and geomtry in normal and pathological neuronal function. *The Neuroscientist* 3:28–41.

Tabata, T. 1990. Ephaptic transmission and conduction velocity of an action potential in *Chara* internodal cells placed in parallel and in contact with one another. *Plant Cell Physiol.* 31:575–579.

Terzuolo, C. A., and Araki, T. 1961. An analysis of intra- versus extracellular potential changes associated with activity of single spinal motoneurons. *Ann. NY Acad. Sci.* 94:547–558.

Tranchina, D., and Nicholson, C. 1986. A model for the polarization of neurons by extrinsically applied electric fields. *Biophys. J.* 50:1139–1156.

Traub, R. D., Dudek, F. E., Snow, R. W., and Knowles, W. D. 1985a. Computer simulations indicate that electrical field effects contribute to the shape of the epileptiform field potential. *Neurosci.* 15:947–958.

Traub, R. D., Dudek, F. E., Taylor, C. P., and Knowles, W. D. 1985b. Simulation of hippocampal afterdischarges synchronized by electrical interaction. *Neurosci.* 14:1033–1038.

Trayanova, N. A., Henriquez, C. S., and Plonsey, R. 1990. Limitations of approximate solutions for computing the extracellular potential of single fibers and bundle equivalents. *IEEE Trans. Biomed. Eng.* 37:22–35.

Trayanova, N., and Henriquez, C. S. 1991. Examination of the choice of models for computing the extracellular potential of a single fibre in a restricted volume conductor. *Med. & Biol. Eng. & Comput.* 29:580–584.

Turner, R. W., and Richardson, T. L. 1991. Apical dendritic depolarizations and field interactions evoked by stimulation of afferent inputs to rat hippocampal CA1 pyramidal cells. *Neurosci.* 42:125–135.

Van Harreveld, A. 1972. The extracellular space in the vertebrate central nervous system. In: *The Structure and Function of Nervous Tissue.* Bourne, G. H., ed., pp. 447-511. Academic Press.

Appendix: Finite or bent axons, cells, and dendrites

Neural elements are straight for long distances only in nerve tracts. In neuropil, where interactions are potentially more interesting, it is important to consider neural elements with sharp bends, terminations, and branches. The effect of the extracellular potential is mediated by the derivative of its gradient in the direction of the axon or dendrite, and the gradient changes abruptly when the direction of the axon or dendrite changes. Therefore the largest effects can be seen at bends in neural processes (Markin, 1973b; Tranchina and Nicholson, 1986).

The modified cable equation 3 must be rewritten in terms of an arc length parameter s instead of distance z, where the cable is described parametrically by $x = x(s)$, $y = y(s)$, $z = z(s)$. With this modification, summing the currents into the node in figure 7 gives

$$\begin{aligned} c_m \frac{\partial V_m}{\partial t} + g_m V_m &= \frac{\partial}{\partial s}\left(\frac{1}{r_i}\frac{\partial V_i}{\partial s}\right) \\ &= \frac{\partial}{\partial s}\left(\frac{1}{r_i}\frac{\partial V_m}{\partial s}\right) + \frac{\partial}{\partial s}\left(\frac{1}{r_i}\frac{\partial V_e}{\partial s}\right) \end{aligned} \tag{8}$$

As discussed previously, this is the standard cable equation except there is a distributed current (the ephaptic current) injected into the cell of magnitude

$$i_{eph} = \frac{\partial}{\partial s}\left(\frac{1}{r_i}\frac{\partial V_e}{\partial s}\right) = \left(\frac{\partial}{\partial s}\frac{1}{r_i}\right)\frac{\partial V_e}{\partial s} + \frac{1}{r_i}\frac{\partial^2 V_e}{\partial s^2} \tag{9}$$

per unit length. The derivatives of the extracellular potential at the surface of the cable V_e depends on the extracellular potential ϕ and the shape of the cable:

$$\frac{\partial V_e}{\partial s} = \nabla\phi \cdot \mathbf{T} = -\mathbf{E} \cdot \mathbf{T} \tag{10}$$

where $\mathbf{E}$ is the electric field and $\mathbf{T}$ is the normalized tangent vector,

$$\mathbf{T} = \left(\frac{dx}{ds}, \frac{dy}{ds}, \frac{dz}{ds}\right). \tag{11}$$

The effective current is proportional to the second derivative,

$$\frac{\partial^2 V_e}{\partial s^2} = -\mathbf{T} \cdot \frac{\partial(E_x, E_y, E_z)}{\partial(x, y, z)}\mathbf{T} - \mathbf{E} \cdot \frac{d\mathbf{T}}{s} \tag{12}$$

where $\partial(E_x, E_y, E_z)/\partial(x, y, z)$ is the Jacobian of $\mathbf{E}$ (the Hessian of $-\phi$).

Axons and dendrites in neuropil tend to have kinks rather than smooth bends, so $\mathbf{T}$ is discontinuous and $d\mathbf{T}/ds$ is a sum of δ functions. As a result, the current source consists of a distributed current (the first term in equation 12) and a series of point current sources at each bend (the second term). The magnitude of each point current source is

$$I_{eph} = -\mathbf{E} \cdot \left(\frac{\mathbf{T}(s^+)}{r_i(s^+)} - \frac{\mathbf{T}(s^-)}{r_i(s^-)}\right) \tag{13}$$

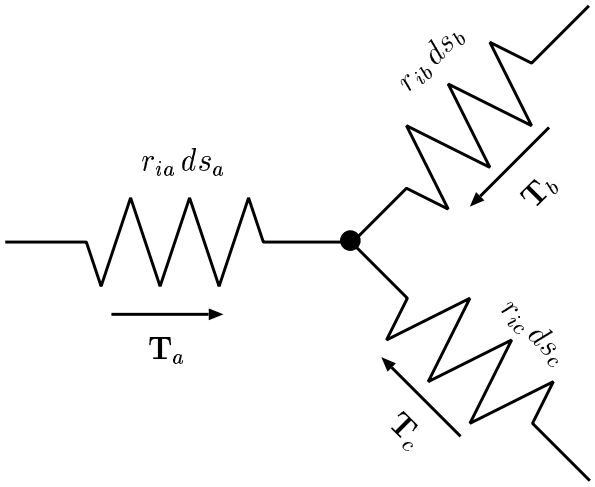

Figure 10: Calculation of ephaptic current at a branch point.

---

where $\mathbf{T}(s^+)$ and $\mathbf{T}(s^-)$ are the tangent vectors on each side of the kink.
A similar situation occurs at a branch point. Summing the currents into the node in figure 10 gives

$$\frac{1}{r_{ia}}\frac{\partial V_{ia}}{\partial s_a} + \frac{1}{r_{ib}}\frac{\partial V_{ib}}{\partial s_b} + \frac{1}{r_{ic}}\frac{\partial V_{ic}}{\partial s_c} = 0, \tag{14}$$

or

$$\frac{1}{r_{ia}}\left(\frac{\partial V_{ma}}{\partial s_a} + \frac{\partial V_{ea}}{\partial s_a}\right) + \frac{1}{r_{ib}}\left(\frac{\partial V_{mb}}{\partial s_b} + \frac{\partial V_{eb}}{\partial s_b}\right) + \frac{1}{r_{ic}}\left(\frac{\partial V_{mc}}{\partial s_c} + \frac{\partial V_{ec}}{\partial s_c}\right) = 0. \tag{15}$$

Therefore, if we consider the transmembrane potential instead of intracellular potential, there is an effective point current source of magnitude

$$\begin{aligned} I_{eph} &= -\frac{1}{r_a}\frac{\partial V_{ea}}{\partial s_a} - \frac{1}{r_b}\frac{\partial V_{eb}}{\partial s_b} - \frac{1}{r_c}\frac{\partial V_{ec}}{\partial s_c} \\ &= \frac{1}{r_a}\mathbf{E}\cdot\mathbf{T}_a + \frac{1}{r_b}\mathbf{E}\cdot\mathbf{T}_b + \frac{1}{r_c}\mathbf{E}\cdot\mathbf{T}_c \end{aligned} \tag{16}$$

injected at the node, in addition to the distributed current source from the Jacobian of $\mathbf{E}$. There is also an effective current at the ends of axons or dendrites. At the end of the cable, no intracellular axial current flows (sealed end condition):

$$\frac{1}{r_i}\frac{\partial V_i}{\partial s} = 0 = \frac{1}{r_i}\left(\frac{\partial V_m}{\partial s} + \frac{\partial V_e}{\partial s}\right). \tag{17}$$

Once again, in terms of V_m, it is as if there is a point current source of magnitude

$$I_{eph} = -\frac{1}{r_i}\frac{\partial V_e}{\partial s} = \frac{1}{r_i}\mathbf{E}\cdot\mathbf{T} \tag{18}$$

located at the end, in addition to the distributed current source.
These special cases are all subsumed by a general rule: at any point along the cable, there is a point current source due to a geometrical inhomogineity at that point which is

$$I_{eph} = \sum \frac{1}{r_i} \mathbf{E} \cdot \mathbf{T} \tag{19}$$

summed over all of the cable segments that join at that point. The direction of $\mathbf{T}$ is taken as toward the point. This rule is also applicable for discontinuous changes in r_i. In addition, there is a distributed current source due to changes in the electrical field at that point,

$$i_{eph} = -\mathbf{T} \cdot \frac{\partial(E_x, E_y, E_z)}{\partial(x, y, z)} \mathbf{T} \tag{20}$$

How much influence do the geometrical irregularities have? Extracellular potentials produced by cell spiking, at least from this particular pyramidal cell model, change very rapidly in space, and the induced transmembrane potential is already almost equal to the extracellular potential (see above); V_m cannot grow any larger. Discontinuities would be more important for less localized potential, perhaps around other cells. For such fields, discontinuities focus the effects of the electrical field and are likely to be important. For example, if electrical stimulation causes an action potential, it is much more likely to initiate at a discontinuity (Tranchina and Nicholson, 1986).